JOURNAL OF COMPUTATIONAL PHYSICS 28, 297–314 (1978)

Calculation of the Flow between Two Rotating Spheres by the Method of Series Truncation

S. C. R. DENNIS

Department of Applied Mathematics, University of Western Ontario, London, Canada N6A 5B9

AND

S. N. SINGH

Department of Mechanical Engineering, University of Kentucky, Lexington, Kentucky 40506

Received June 1, 1977; revised September 27, 1977

A numerical method is described for solving three coupled sets of nonlinear ordinary differential equations of the second order which arise in the study of the steady axially symmetric motion of an incompressible viscous fluid contained between two concentric rotating spheres. The flow variables are expressed as series of orthogonal Gegenbauer functions with variable coefficients, thus reducing the equations of motion to ordinary differential equations with two-point boundary conditions. The boundary conditions for the stream function are utilized to obtain an integral condition which permits one of the sets of equations to be solved using step-by-step methods. Numerical solutions are obtained for values up to 2000 of the Reynolds number based on the radius of the outer sphere. Results for the stream function and the torque required to rotate the spheres are compared with those obtained by previous investigators.

1. INTRODUCTION

The problem of finding the motion of a viscous fluid between two concentric spheres rotating about a common axis with different angular velocities has recently drawn considerable attention because of its interest in engineering design and geophysics. Singular perturbation solutions for large Reynolds number have been presented by Bondi and Lyttleton [1], Proudman [2], Carrier [3], Stewartson [4] and Pedlosky [5]. For small Reynolds numbers, Haberman [6], Ovseenko [7], Langlois [8] and Munson and Joseph [9] attempted solutions in powers of the Reynolds number. Munson and Joseph also determined the basic flow at higher Reynolds numbers by using a series truncation method in terms of Legendre polynomials. Pearson [10] calculated the time-dependent rotationally symmetric motion for cases in which one (or both) of the spheres is given an impulsive change in angular velocity, starting from a state of either rest or uniform rotation, for Reynolds numbers from 10 to 1500. Recently

0021-9991/78/0283–0297$02.00/0

Greenspan [11] integrated numerically the steady-state equations and presented the results in the form of streamlines for a range of Reynolds numbers up to 3000.

In the present paper, we describe details of a method of solving problems involving axially symmetric flow between rotating spheres by means of series truncation. The basic method was proposed by Van Dyke [12], [13] and an application to calculate the steady flow past a circular cylinder at small Reynolds numbers was given by Underwood [14]. Dennis and Walker [15] applied a similar method to the calculation of steady flow past a sphere, but using quite different numerical procedures and a different method of satisfying the boundary conditions in which an integral involving the vorticity was employed. A similar type of integral condition had been used by Dennis and Chang [16] in calculating steady flow past a circular cylinder and, subsequently, Collins and Dennis [17] used a time-dependent integral condition in studying flow past an impulsively started circular cylinder. The use of appropriate integral conditions is a feature of the present method also. The important point underlying the use of these conditions is that the stream function is determined by step-by-step integrations rather than by boundary-value methods.

The stream function and other flow variables are expanded in series of orthogonal Gegenbauer functions in terms of the angle θ of spherical polar coordinates (r, θ, ϕ), the motion being independent of the angle ϕ. The series have coefficients which are functions of the radial variable r and on substitution in the Navier–Stokes equations it is possible to derive three sets of second-order ordinary differential equations for the functional coefficients subject to two-point boundary conditions. The equations are truncated by putting all functional coefficients after a certain stage in the series equal to zero. The finite set of equations which results from the truncation process is solved by a specialized numerical scheme. The difference between the present approach and the method of series truncation used by Munson and Joseph is that they used series of Legendre polynomials rather than Gegenbauer functions. The latter functions are found to be more appropriate, by virtue of their different orthogonality properties, to the differential operators which occur in the present problem. The method employed by Munson and Joseph for solving the differential equations and utilizing the boundary conditions is also different.

The problem is formulated for the general case of flow between an inner sphere of radius r_1 rotating with angular velocity Ω_1 about a fixed diameter and a concentric outer sphere of radius r_2 rotating about the same diameter with angular velocity Ω_2. A Reynolds number R is based on the radius of the outer sphere and some typical angular velocity Ω_0 and is defined by $R = r_2{}^2\Omega_0/\nu$, where ν is the coefficient of kinematic viscosity. Calculations have been carried out assuming $r_2 = 2r_1$ and for Reynolds numbers $R = 100$, 500, 1000 and 2000 in each of two cases. In one of these the inner sphere rotates with the outer one at rest giving $\Omega_1 = \Omega_0$, $\Omega_2 = 0$. In the second the outer sphere rotates with the inner one at rest corresponding to $\Omega_1 = 0$, $\Omega_2 = \Omega_0$. The streamlines of the motion are compared where possible with those calculated by Pearson [10] at large times after an impulsive start of the motion. Comparison is also made with the steady-state solutions of Greenspan [11]. The torque required to rotate the moving sphere in either case is calculated. Munson and

Joseph [9] calculated the torque up to $R = 1000$ and the comparison is found to be good. Finally, it may be noted that the methods of the present paper can be applied with some modification to several problems of interest including that of a single rotating sphere in a fluid at rest as well as the case of a translating sphere in a rotating fluid.

2. Basic Equations and Analysis

We consider the steady flow of a viscous incompressible fluid occupying the region between two concentric spheres which are rotating about a common axis through the centre. The flow is assumed to be symmetrical about the axis of rotation which is taken as the axis $\theta = 0$ of spherical polar coordinates (r, θ, ϕ) with origin at the centre of the spheres, and hence all quantities are independent of ϕ. We introduce the transformation $\xi = \ln(r/r_2)$, where r_2 is the radius of the outer sphere, and then we can relate the dimensionless velocity components (v_r, v_θ, v_ϕ) to the dimensionless functions ψ and Ω by the relations

$$v_r = \frac{e^{-2\xi}}{\sin\theta}\frac{\partial\psi}{\partial\theta}, \qquad v_\theta = -\frac{e^{-2\xi}}{\sin\theta}\frac{\partial\psi}{\partial\xi}, \qquad v_\phi = \frac{\Omega e^{-\xi}}{\sin\theta}. \tag{1}$$

Here ψ is the dimensionless stream function. The Navier–Stokes equations governing the motion can then be written (see [2, 9]) in the form

$$D^2\Omega = \frac{Re^{-\xi}}{\sin\theta}\left(\frac{\partial\psi}{\partial\theta}\frac{\partial\Omega}{\partial\xi} - \frac{\partial\psi}{\partial\xi}\frac{\partial\Omega}{\partial\theta}\right), \tag{2}$$

$$D^2\psi = -e^{2\xi}\zeta, \tag{3}$$

$$\begin{aligned} D^2\zeta = \frac{Re^{-\xi}}{\sin\theta}\Big[&\frac{\partial\psi}{\partial\theta}\frac{\partial\zeta}{\partial\xi} - \frac{\partial\psi}{\partial\xi}\frac{\partial\zeta}{\partial\theta} \\ &+ 2\left\{\left(\cot\theta\frac{\partial\psi}{\partial\xi} - \frac{\partial\psi}{\partial\theta}\right)\zeta - \left(\cot\theta\frac{\partial\Omega}{\partial\xi} - \frac{\partial\Omega}{\partial\theta}\right)\Omega\right\}\Big], \end{aligned} \tag{4}$$

where

$$D^2 = \frac{\partial^2}{\partial\xi^2} - \frac{\partial}{\partial\xi} + \sin\theta\frac{\partial}{\partial\theta}\left(\frac{1}{\sin\theta}\frac{\partial}{\partial\theta}\right).$$

If the actual physical dependent variables are denoted by starred quantities, the dimensional velocity components are given by

$$v_r^* = \frac{\partial\psi^*/\partial\theta}{r^2\sin\theta}, \qquad v_\theta^* = \frac{-\partial\psi^*/\partial r}{r\sin\theta}, \qquad v_\phi^* = \frac{\Omega^*}{r\sin\theta}, \tag{5}$$

where

$$\psi^* = r_2{}^3\Omega_0\psi, \qquad \Omega^* = r_2{}^2\Omega_0\Omega, \tag{6}$$

and Ω_0 is a representative angular velocity. This could be taken as the angular velocity of either sphere. The Reynolds number is defined by $R = r_2{}^2\Omega_0/\nu$, where ν is the coefficient of kinematic viscosity.

In the following we associate angular velocities Ω_1 and Ω_2 with the inner and outer spheres respectively and denote by ξ_0 the value of ξ at the inner sphere $r = r_1$. Thus in terms of the quantities

$$\omega_1 = 2r_1{}^2\Omega_1/r_2{}^2\Omega_0, \qquad \omega_2 = 2\Omega_2/\Omega_0, \qquad \xi_0 = \ln(r_1/r_2), \tag{7}$$

the boundary conditions can be stated as

$$\psi = \partial\psi/\partial\xi = 0 \qquad \text{when} \quad \xi = \xi_0 \quad \text{and} \quad \xi = 0, \tag{8}$$

$$\left.\begin{aligned} \Omega &= \tfrac{1}{2}\omega_1 \sin^2\theta \qquad \text{when} \quad \xi = \xi_0; \\ \Omega &= \tfrac{1}{2}\omega_2 \sin^2\theta \qquad \text{when} \quad \xi = 0. \end{aligned}\right. \tag{9}$$

In order to apply the series truncation method we now assume the expansions

$$\Omega = \sum_{n=1}^{\infty} I_{2n}(\mu) f_n(\xi), \tag{10}$$

$$\psi = \sum_{n=1}^{\infty} I_{2n+1}(\mu)\, g_n(\xi), \tag{11}$$

$$\zeta = \sum_{n=1}^{\infty} I_{2n+1}(\mu)\, h_n(\xi), \tag{12}$$

where $\mu = \cos\theta$ and $I_n(\mu)$ are the Gegenbauer functions of the first kind and of order n (see [18, 19]). The functions $I_n(\mu)$ are appropriate to the operator D^2 which appears in (2)–(4) because of their orthogonality properties. They are even or odd functions of μ accordingly as n is even or odd, and the appearance of only even or odd functions in each of the expansions (10)–(12) reflects the symmetry of Ω and antisymmetry of ψ and ζ about $\theta = \pi/2$.

If the expansions (11) and (12) are substituted into (3) we obtain the infinite set of equations

$$g_n'' - g_n' - 2n(2n+1)\, g_n = -e^{2\xi}h_n, \tag{13}$$

which hold for positive integer values of n, where the prime denotes differentiation with respect to ξ. The conditions (8) on ψ become

$$g_n(\xi_0) = g_n(0) = 0; \qquad g_n'(\xi_0) = g_n'(0) = 0. \tag{14}$$

If we introduce the substitution

$$g_n = e^{\xi/2}G_n \tag{15}$$

into (13), we get the set of equations

$$G_n'' - k^2 G_n = -e^{3\xi/2} h_n = r_n\,, \tag{16}$$

where $k = (2n + \frac{1}{2})$. The corresponding boundary conditions are

$$G_n(\xi_0) = G_n(0) = 0; \qquad G_n'(\xi_0) = G_n'(0) = 0. \tag{17}$$

We now multiply (16) by $e^{\pm k\xi}$ and integrate it with respect to ξ from $\xi = \xi_0$ to $\xi = 0$. In view of (17) we obtain

$$\int_{\xi_0}^{0} r_n e^{\pm k\xi}\, d\xi = 0 \qquad \text{for all } n. \tag{18}$$

The set of conditions (18) for positive integer values of n is in effect two sets obtained by taking the positive and negative signs in the exponential. We shall describe later how (18) may be employed to calculate $r_n(\xi_0)$ and $r_n(0)$ for a given value of n. This determines $h_n(\xi_0)$ and $h_n(0)$ by the equality defined in (16) and then it is possible to construct a simple step-by-step procedure to determine $G_n(\xi)$ in which all of (17) are finally satisfied.

If the expressions (10)–(12) for Ω, ψ and ζ are substituted into (2) and (4), it is found by standard methods of orthogonal functions that we can derive two sets of ordinary differential equations of the form

$$f_n'' + (A_n - 1) f_n' - \{2n(2n - 1) + B_n\} f_n = R_n\,, \tag{19}$$

$$h_n'' + (C_n - 1) h_n' - \{2n(2n + 1) + D_n\} h_n = S_n\,. \tag{20}$$

Thus the set of equations (19) is obtained by expressing (2) in terms of the variable μ, dividing each side by $1 - \mu^2$, multiplying by the general term of (10) and integrating with respect to μ from $\mu = -1$ to $\mu = 1$. A similar procedure is used to obtain the set (20). In both cases it is necessary to utilize the orthogonality properties of the functions $I_n(\mu)$. These are briefly noted in an appendix to the present paper together with a brief note on some formulas for the evaluation of integrals involving triple products of Gegenbauer functions which are given next.

The quantities $A_n(\xi)$, $B_n(\xi)$, $R_n(\xi)$ in (19) and $C_n(\xi)$, $D_n(\xi)$, $S_n(\xi)$ in (20) can all be expressed in terms of the functions $f_n(\xi)$, $g_n(\xi)$, $h_n(\xi)$ and the quantities $L(l, m, n)$ and $M(l, m, n)$ defined by

$$L(l, m, n) = \frac{1}{2}\int_{-1}^{1} \frac{I_{l+1}(\mu)\, I_{m+1}(\mu)\, I_{n+1}'(\mu)}{1 - \mu^2}\, d\mu, \tag{21}$$

$$M(l, m, n) = \int_{-1}^{1} \frac{\mu I_{l+1}(\mu)\, I_{m+1}(\mu)\, I_{n+1}(\mu)}{(1 - \mu^2)^2}\, d\mu, \tag{22}$$

where the prime in (21) denotes differentiation with respect to μ. It may be shown (see appendix) from the basic results described by Talman [20] that

$$L(l, m, n) = [l(l+1)\, m(m+1)]^{-1/2} \begin{pmatrix} l & m & n \\ 1 & -1 & 0 \end{pmatrix} \begin{pmatrix} l & m & n \\ 0 & 0 & 0 \end{pmatrix}, \tag{23}$$

$$M(l, m, n) = \left[\frac{(l-1)(l+2)}{lmn(l+1)(m+1)(n+1)}\right]^{1/2} \times \begin{pmatrix} l & m & n \\ -1 & -1 & 2 \end{pmatrix} \begin{pmatrix} l & m & n \\ 0 & 0 & 0 \end{pmatrix} - L(l, m, n), \tag{24}$$

where

$$\begin{pmatrix} j_1 & j_2 & j_3 \\ m_1 & m_2 & m_3 \end{pmatrix}$$

are the $3-j$ symbols.

A table of $3-j$ symbols and the algorithm to compute them numerically is given by Rotenberg *et al.* [21].

Expressions for the coefficients in (19) and (20) may now be given as

$$A_n = Re^{-\xi} a_n \sum_{m=1}^{\infty} L(2n-1, 2n-1, 2m)\, g_m\,, \tag{25}$$

$$B_n = Re^{-\xi} a_n \sum_{m=1}^{\infty} L(2m, 2n-1, 2n-1)\, g'_m\,, \tag{26}$$

$$C_n = Re^{-\xi} b_n \sum_{l=1}^{\infty} L(2n, 2n, 2l)\, g_l\,, \tag{27}$$

$$D_n = Re^{-\xi} b_n \sum_{l=1}^{\infty} [2L(2n, 2n, 2l)\, g_l + \{L(2l, 2n, 2n) + M(2l, 2n, 2n)\}\, g'_l], \tag{28}$$

$$R_n = Re^{-\xi} a_n \sum_{l=1}^{\infty} \sum_{m=1}^{\infty} \{L(2m, 2n-1, 2l-1)\, f_l g'_m - L(2l-1, 2n-1, 2m)\, f'_l g_m\} - B_n f_n + A_n f'_n\,, \tag{29}$$

$$S_n = Re^{-\xi} b_n \sum_{l=1}^{\infty} \sum_{m=1}^{\infty} [\{L(2l, 2n, 2m)\, g'_l h_m - L(2m, 2n, 2l)\, g_l h'_m\} + \{2L(2m, 2n, 2l)\, g_l + M(2l, 2m, 2n)\, g'_l\}\, h_m - \{2L(2l-1, 2n, 2m-1)\, f_l + M(2l-1, 2m-1, 2n)\, f'_l\}\, f_m] - D_n h_n + C_n h'_n\,. \tag{30}$$

In all of these formulas

$$a_n = 2n(2n-1)(4n-1), \qquad b_n = 2n(2n+1)(4n+1). \tag{31}$$

A set of boundary conditions for Eqs. (19) may be obtained by substituting expansion (10) into conditions (9), from which it is found that

$$f_1(\xi_0) = \omega_1\,, \quad f_1(0) = \omega_2\,; \qquad f_n(\xi_0) = f_n(0) = 0 \quad \text{for } n > 1. \tag{32}$$

There are no direct boundary conditions for (20), but values of $h_n(\xi_0)$ and $h_n(0)$ may be found indirectly by satisfying the set of integral conditions (18). The theoretical problem is now to solve the sets of equations (16), (19), and (20) subject to conditions (17), (18), and (32). In practice the sets of equations must be truncated. A truncation of order n_0 is defined by putting all functions in the expansions (10)–(12) with subscripts $n > n_0$ identically equal to zero and solving the $3n_0$ second-order differential equations with associated boundary conditions which result. Numerical solutions are obtained by an iterative procedure, details of which are described in the next section.

3. Numerical Methods

The equations are solved numerically by the usual procedure of dividing the range $\xi = \xi_0$ to $\xi = 0$ into p intervals of uniform grid size h. Each equation of the truncated sets (19) and (20) is solved by approximating all derivatives by means of standard three-point central-difference formulas. Thus at a general point ξ the approximation to (19) can be written as

$$\begin{aligned}[1 - \tfrac{1}{2}h\{A_n(\xi) - 1\}]\,f_n(\xi - h) &- [2 + h^2\{2n(2n-1) + B_n(\xi)\}]\,f_n(\xi) \\ &+ [1 + \tfrac{1}{2}h\{A_n(\xi) - 1\}]\,f_n(\xi + h) = h^2 R_n(\xi).\end{aligned} \tag{33}$$

Approximations to $A_n(\xi)$, $B_n(\xi)$ and $R_n(\xi)$ are known at every internal grid point during the course of the iterative method. At a given stage the tridiagonal matrix problem associated with (33) subject to the conditions (32) is solved by the stable direct method described by Rosser [22]. A typical equation of set (20) is likewise approximated by

$$\begin{aligned}[1 - \tfrac{1}{2}h\{C_n(\xi) - 1\}]\,h_n(\xi - h) &- [2 + h^2\{2n(2n+1) + D_n(\xi)\}]\,h_n(\xi) \\ &+ [1 + \tfrac{1}{2}h\{C_n(\xi) - 1\}]\,h_n(\xi + h) = h^2 S_n(\xi),\end{aligned} \tag{34}$$

and this set of equations is solved for $h_n(\xi)$ by the same method with boundary conditions

$$h_n(\xi_0) = \alpha_n\,, \qquad h_n(0) = \beta_n\,, \tag{35}$$

where α_n and β_n are calculated from (18) in the manner which follows.

The condition obtained by taking the positive exponent in (18) is

$$\int_{\xi_0}^{0} r_n e^{k\xi}\, d\xi = 0. \tag{36}$$

If (36) is expressed as a quadrature formula in the range $\xi = \xi_0$ to $\xi = 0$, we get the approximation

$$c_0 r_n(\xi_0) + c_1 r_n(\xi_0 + h) + \cdots + c_p r_n(0) = 0$$

or

$$c_0 r_n(\xi_0) + c_p r_n(0) + Q = 0, \tag{37}$$

where c_n are the coefficients of the quadrature formula (outlined below) and Q is the sum over internal values. Similarly the second integral (18) with the negative exponent gives

$$c_0' r_n(\xi_0) + c_p' r_n(0) + Q' = 0. \tag{38}$$

We can now solve (37) and (38) to get

$$r_n(\xi_0) = (c_p Q' - c_p' Q)/(c_0 c_p' - c_0' c_p), \tag{39}$$

$$r_n(0) = (c_0' Q - c_0 Q')/(c_0 c_p' - c_0' c_p), \tag{40}$$

and hence α_n and β_n from (35), since $r_n = -h_n e^{3\xi/2}$.

We could use any suitable quadrature formula to give the c_n, for example Simpson's rule by taking p to be even. However, we use a specialized formula based on Simpson's rule, in which we deal with the integrand $r_n e^{k\xi}$ in (36) by replacing r_n by a parabola over three consecutive points and then integrating by parts. This procedure is much better than replacing $r_n e^{k\xi}$ by a parabola because this latter function varies extremely rapidly with ξ when k is only moderately large, whereas r_n varies relatively slowly. Thus by replacing r_n by a parabola over three consecutive points we can get accurate values of the integral in (36) even if k is large. In effect this means that we can use the same grid size h to approximate the condition (36) accurately for any value of k. The same principle holds for any type of polynomial approximation to r_n but we shall confine ourselves to the case of a second-degree polynomial here.

If we suppress the subscript on r_n for the moment and assume that with a uniform grid h

$$r(\xi) = a + b\xi + c\xi^2 \tag{41}$$

over any three successive values ξ_1, ξ_2, ξ_3 of ξ, we easily find that

$$\int_{\xi_1}^{\xi_3} r e^{k\xi}\, d\xi = \frac{1}{k}\left[r_3 e^{k\xi_3} - r_1 e^{k\xi_1}\right] - \frac{1}{k^2}\left[(b + 2c\xi_3)\, e^{k\xi_3} - (b + 2c\xi_1)\, e^{k\xi_1}\right] + \frac{2c}{k^3}\left(e^{k\xi_3} - e^{k\xi_1}\right). \tag{42}$$

A similar formula holds for the definite integral from $\xi = \xi_1$ to $\xi = \xi_2$ by replacing ξ_3 by ξ_2 in (42). In either case we fit (41) to the values r_1, r_2 and r_3 of r at $\xi = \xi_1$, $\xi = \xi_2$ and $\xi = \xi_3$ to obtain

$$\begin{aligned} b + 2c\xi_1 &= (4r_2 - 3r_1 - r_3)/2h, & b + 2c\xi_2 &= (r_3 - r_1)/2h, \\ b + 2c\xi_3 &= (r_1 - 4r_2 + 3r_3)/2h, & c &= (r_1 - 2r_2 + r_3)/2h^2. \end{aligned} \tag{43}$$

With the necessary substitutions from (43), the formula (42) is now used to obtain (37) by applying it to each consecutive pair of intervals from $\xi = \xi_0$ to $\xi = 0$ and summing, assuming p to be even. We need only change the sign of k in (42) for it to be appropriate to the second integral in (18) with the negative exponent and a similar procedure of summing gives (38). It follows from (42) and (43) that

$$e^{-k\xi_0}c_0 = c_p' = -\frac{1}{k} - \frac{1}{2hk^2}(3 + e^{2kh}) - \frac{1}{h^2k^3}(1 - e^{2kh}), \tag{44}$$

$$e^{k\xi_0}c_0' = c_p = \frac{1}{k} - \frac{1}{2hk^2}(3 + e^{-2kh}) + \frac{1}{h^2k^3}(1 - e^{-2kh}). \tag{45}$$

Hence from an approximation to $h_n(\xi)$, and thus $r_n(\xi)$, at internal grid points we can calculate an approximation to α_n and β_n in (35).

When this approximation to α_n and β_n has been calculated for a given n, the function $r_n(\xi)$ is known approximately at all grid points including $\xi = \xi_0$ and $\xi = 0$. We can now integrate Eqs. (16) by step-by-step methods, by introducing the functions defined by

$$u = G' - kG, \qquad v = G' + kG, \tag{46}$$

and then u and v satisfy

$$u' + ku = r, \qquad v' - kv = r, \tag{47}$$

where the subscripts on the functions G_n and r_n have again been dropped temporarily for convenience. It follows from (17) that the boundary conditions for u and v are

$$u = v = 0, \qquad \text{when} \qquad \xi = \xi_0 \qquad \text{and} \qquad \xi = 0. \tag{48}$$

If the first equation of (47) is multiplied by $e^{k\xi}$ and integrated over the range covered by the three successive points ξ_1, ξ_2 and ξ_3 we obtain

$$u_3 = \gamma^2 u_1 + e^{-k\xi_3}\int_{\xi_1}^{\xi_3} re^{k\xi}\, d\xi, \tag{49}$$

where $\gamma = e^{-kh}$. We now utilize (42) and then the whole of the last term on the right side of (49) can be replaced by the right side of (42) with $e^{k\xi_3}$ replaced by unity and $e^{k\xi_1}$ replaced by γ^2. This gives a step-by-step formula to construct a numerical solution for u at all grid points starting from $u(\xi_0)$ and $u(\xi_0 + h)$ and it is stable since $\gamma < 1$. Moreover we can obtain $u(\xi_0 + h)$ from the known value $u(\xi_0) = 0$ by employing a formula similar to (49) in which u_3 and ξ_3 are replaced by u_2 and ξ_2 respectively and γ^2 is replaced by γ. The necessary integral from $\xi = \xi_1$ to $\xi = \xi_2$ is then found by replacing ξ_3 by ξ_2 in (42) and using the second of (43). Finally it is easily shown that repeated application of (49) starting from $u(\xi_0) = 0$ must lead to $u(0) = 0$ provided that (36) has been satisfied. This gives a check on the numerical procedures.

Just as the stable direction of integration of the first of (47) is the direction of increasing ξ, the stable direction for the second of (47) is that of decreasing ξ. If we multiply the second equation of (47) by $e^{-k\xi}$ and integrate from $\xi = \xi_1$ to $\xi = \xi_3$ we find that

$$v_1 = \gamma^2 v_3 - e^{k\xi_1} \int_{\xi_1}^{\xi_3} re^{-k\xi}\, d\xi, \tag{50}$$

and the integral is given by (42) with the sign of k changed. This stable formula can be used to construct a numerical solution for v starting from $v(0)$ and $v(-h)$. A formula to get $v(-h)$ from $v(0)$ is obtained from (50) by replacing v_1, ξ_1 and γ^2 by v_2, ξ_2 and γ respectively. The necessary integral is obtained from (42) by replacing ξ_1 by ξ_2. Again the solution for v obtained by repeated application of (50) starting with $v(0) = 0$ will come out to be zero at $\xi = \xi_0$ if the condition (18) with the negative exponent has been satisfied. From the solutions for u and v we obtain both G and G' from (46). The method is very rapid since it requires no iteration. Some further details have been discussed by Dennis and Chang [23].

The iterative sequence of steps of solving the various equations for a given truncation is carried out by constructing sets of approximations $f_n^{(m)}(\xi)$, $g_n^{(m)}(\xi)$, $h_n^{(m)}(\xi)$ $(n = 1, 2,..., n_0)$, starting from an initial set corresponding to $m = 0$. When this has been completed to stage m the following steps are carried out to complete the next stage. The set of equations (19) is solved subject to (32) by matrix inversion using the most recently available information for $A_n(\xi)$, $B_n(\xi)$ and $R_n(\xi)$. Each solution member which results is denoted by $f_n^{(m+1/2)}(\xi)$ and then the next approximation is defined by

$$f_n^{(m+1)}(\xi) = Kf_n^{(m+1/2)}(\xi) + (1 - K) f_n^{(m)}(\xi) \qquad (n = 1, 2,..., n_0). \tag{51}$$

Here K is an empirically chosen parameter in the range $0 < K \leqslant 1$. The set of equations (20) is now solved subject to the most recent estimates of α_n and β_n in (35) and with the most recently available data for $C_n(\xi)$, $D_n(\xi)$ and $S_n(\xi)$. A solution member is again denoted by $h_n^{(m+1/2)}(\xi)$ and the next approximation is defined by

$$h_n^{(m+1)}(\xi) = Kh_n^{(m+1/2)}(\xi) + (1 - K) h_n^{(m)}(\xi) \qquad (n = 1, 2,..., n_0). \tag{52}$$

Revised estimates of α_n and β_n are now obtained by satisfying (18) in the manner already described and the set of equations (16) is then solved. Each equation is solved in sequence by the given step-by-step method and thus from (15) we arrive at the set of functions $g_n^{(m+1)}(\xi)$ $(n = 1, 2,..., n_0)$. This ends one complete cycle of the iterative procedure.

The sequence of iterations is continued by repeating this cycle until convergence is obtained. This is described by the test

$$| h_n^{(m+1)}(\xi_0) - h_n^{(m)}(\xi_0)| < \epsilon, \qquad | h_n^{(m+1)}(0) - h_n^{(m)}(0)| < \epsilon \tag{53}$$

for all $n = 1, 2,..., n_0$. Here ϵ is a preassigned tolerance which is a parameter of the solution procedure. The test (53) is completely satisfactory because the boundary values of the functions $h_n(\xi)$ are the last of the properties of the solution to settle down as the iterations proceed so that by the time (53) is satisfied all the functions have converged to acceptable limits throughout the whole solution field. The processes defined by (51) and (52) are, of course, averaging processes and the quantity K is a parameter of the solution. If the iteration procedure tends to be divergent in any given case, a reduction of the value of K often leads to convergence. Generally speaking, K has to be reduced as the Reynolds number increases. The other main parameters of the solutions are the grid size h and the number of terms n_0 which is used to define the truncation. An attempt has been made to determine the effect on the numerical solutions of varying all of these parameters. One of the crucial parameters is obviously the number of terms n_0 utilized in each of the expansions (10)–(12). The parameter n_0 must be increased with increasing Reynolds number for the reason that more terms are required as the flow becomes more complicated. In the calculations carried out the maximum value of n_0 used for a given Reynolds number was based on a balance between obtaining physical properties of reasonable accuracy without an unreasonable amount of computation.

In the results described in the following section a range of Reynolds numbers from $R = 100$ to $R = 2000$ has been covered for the two cases $\Omega_1 = \Omega_0$, $\Omega_2 = 0$ and $\Omega_1 = 0$, $\Omega_2 = \Omega_0$. In every case the solution procedure was started by calculating the first truncation ($n_0 = 1$) and then determining higher truncations by starting from the previous truncation and adding one term to each of (10)–(12), assuming the initial approximation to each new set of terms to be zero. A suitable initial approximation for the first truncation is

$$f_1^{(0)}(\xi) = \omega_2 + (\omega_1 - \omega_2)\,\xi/\xi_0, \qquad g_1^{(0)}(\xi) = 0, \qquad h_1^{(0)}(\xi) = 0 \tag{54}$$

for $\xi_0 \leqslant \xi \leqslant 0$. This was used to start the two cases at $R = 100$. The initial approximation to the first truncation at higher Reynolds numbers was taken as the corresponding final solution at $n_0 = 1$ for the previous value of R.

4. Calculated Results

The results given in the present section were obtained taking the radii of the spheres such that $r_2 = 2r_1$ to facilitate comparison with previous work. This gives $\xi_0 = -\ln 2$. Two quite small grid sizes $h = -\xi_0/80$ and $h = -\xi_0/160$ were used in obtaining numerical solutions, the first for $R \leqslant 500$ and the second for $R \geqslant 500$. The parameters corresponding to the results to be presented are given in Table I.

One of the quantities of interest is the torque which acts on either of the spheres. Munson and Joseph [9] have determined the torque on the spheres in various cases including the two considered here. The torque acting on a given sphere may be found from the expression

$$M^* = \int_{\phi=0}^{2\pi} \int_{\theta=0}^{\pi} r^3 \sin^2 \theta \tau_{\phi r}^* \, d\theta \, d\phi, \tag{55}$$

TABLE I

Parameters of Calculations

R	ω_1	ω_2	$h \times 10^2$	K	$\epsilon \times 10^4$	n_0
100	0.5	0	0.866434	0.06	0.1	5
500	0.5	0	0.433217	0.06	0.1	7
1000	0.5	0	0.433217	0.04	0.1	8
2000	0.5	0	0.433217	0.04	1.0	8
100	0	2.0	0.866434	0.06	0.1	5
500	0	2.0	0.433217	0.04	0.1	6
1000	0	2.0	0.433217	0.04	0.1	7
2000	0	2.0	0.433217	0.04	0.1	7

where $\tau^*_{\phi r}$ is the appropriate component of the stress tensor given by

$$\tau^*_{\phi r} = \rho\nu \left[\frac{1}{r \sin\theta} \frac{\partial v^*_r}{\partial\theta} + r \frac{\partial}{\partial r}\left(\frac{v^*_\phi}{r}\right)\right] \tag{56}$$

and ρ is the density of the fluid. The integral in (55) is taken over either sphere and if we substitute $\partial v^*_r/\partial\theta = 0$ in (56) and utilize (5) and (6) it is found that

$$M^* = 2\pi\rho\nu r_2{}^3\Omega_0 e^\xi \int_0^\pi \left(\frac{\partial\Omega}{\partial\xi} - 2\Omega\right) \sin\theta \, d\theta, \tag{57}$$

where both ξ and the integrand are appropriate to the sphere concerned. A dimensionless coefficient M may now be defined by the relation $M^* = (8\pi/3)\, \rho\nu r_2{}^3\Omega_0 M$. On substitution of this in (57) and use of expansion (10) for Ω the results

$$M_1 = \tfrac{1}{4}\{f_1'(\xi_0) - 2f_1(\xi_0)\}, \qquad M_2 = \tfrac{1}{2}\{f_1'(0) - 2f_1(0)\} \tag{58}$$

are obtained for the coefficients appropriate to the inner and outer spheres respectively, where the ratio $r_2 = 2r_1$ is assumed.

In Table II we give calculated values of M_1 for the case $\Omega_1 = \Omega_0$, $\Omega_2 = 0$ and values of M_2 for the case $\Omega_1 = 0$, $\Omega_2 = \Omega_0$. In both cases the results are based on solutions obtained using the parameters in Table I. Munson and Joseph have given graphical results for $7M_1/3$ up to $R = 1000$ in the first case and for $7M_2/3$ up to about $R = 900$ in the second case. The agreement with the present results is excellent in both cases. For example the numerical value of $7M_1/3$ at $R = 1000$ in the first case is very slightly below 2.3 from Munson and Joseph's graph, while the corresponding value from Table 2 is 2.28. Two checks have been applied to the present results. In the first place the variation of the torque with the order n_0 of the truncation was noted. It was found that when n_0 had reached the values given in Table I the values of M_1 and M_2 given in Table II did actually represent true limits to the precision quoted.

TABLE II

Nondimensional Torque for Rotating Spheres

R	$\Omega_1 = \Omega_0, \Omega_2 = 0$ $-M_1$	$\Omega_1 = 0, \Omega_2 = \Omega_0$ M_2
100	0.446	0.500
500	0.738	0.715
1000	0.978	0.864
2000	1.285	1.069

As a second check the results in both cases at $R = 500$ were obtained using two separate grids $h = -\xi_0/80$ and $h = -\xi_0/160$. For the coarser grid the results comparable with those in Table II were found to be $M_1 = -0.738$, $M_2 = 0.720$ and there was a similar general type of agreement for all properties of the solutions on the two respective grids. The finer grid was therefore judged to be adequate at $R = 500$ and was assumed to be adequate for $R > 500$.

The streamlines of the motion in a plane of constant ϕ were calculated in each of the eight solutions. The effect of the order of the truncation n_0 on the streamlines was studied and it was judged that the results obtained for the values of n_0 given in Table I were adequate except for the one case $R = 2000$, $\Omega_1 = \Omega_0$, $\Omega_2 = 0$. In this case the streamlines did not appear to have reached a consistent pattern at $n_0 = 8$ and one or two further terms would probably be necessary in the series (10)–(12) with considerably more computation. The details of this case have therefore been omitted. It is found that the patterns for the case $R = 100$, $\Omega_1 = \Omega_0$, $\Omega_2 = 0$ agree in character with those given by Greenspan [11, Fig. 4] and those for the case $R = 100$, $\Omega_1 = 0$, $\Omega_2 = \Omega_0$ agree precisely with the results of Pearson [10, Fig. 3] for the essentially steady-state solution. The present details of these cases have been omitted for this reason.

Calculated streamlines for the case $\Omega_1 = \Omega_0$, $\Omega_2 = 0$ are shown for $R = 500$ in Fig. 1 and for $R = 1000$ in Fig. 2. There is excellent agreement between Fig. 2 and the details of the late time solution for the corresponding situation given by Pearson [10, Fig. 10]. The streamlines for $R = 500$, 1000 and 2000 respectively in the case $\Omega_1 = 0, \Omega_2 = \Omega_0$ are given in Figs. 3–5. Once again there is very reasonable agreement between the details of Fig. 4 and the corresponding patterns of the late time solution of Pearson [10, Fig. 4] in both general character and in the magnitude of the stream function. There is no evidence in the present solution for $R = 1000$ of the additional closed streamline found by Greenspan [11, Fig. 9] in the upper part of his diagram for this same case and there are substantial numerical discrepancies in the magnitude of the stream function in several places. Moreover, the general development of the present solution in the region $\theta < 45°$ as R increases from 1000 to 2000 does not appear to be completely consistent with the subsequent development found at

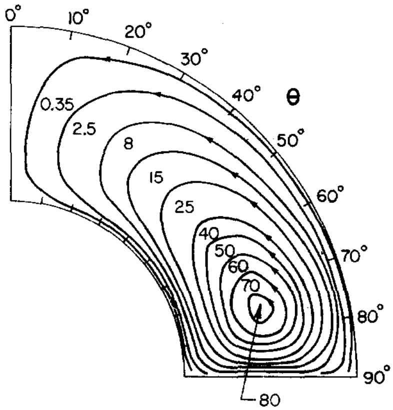

FIG. 1. Contours of $-10^4\psi$ for $R = 500$, $\Omega_1 = \Omega_0$, $\Omega_2 = 0$. The inner sphere rotates and the outer sphere is at rest.

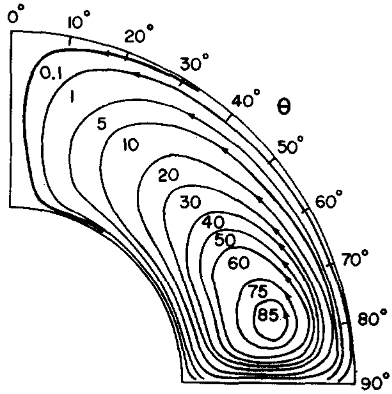

FIG. 2. Contours of $-10^4\psi$ for $R = 1000$, $\Omega_1 = \Omega_0$, $\Omega_2 = 0$.

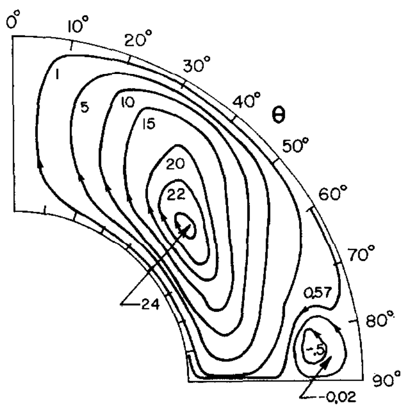

FIG. 3. Contours of $10^4\psi$ for $R = 500$, $\Omega_1 = 0$, $\Omega_2 = \Omega_0$. The inner sphere is at rest and the outer sphere rotates.

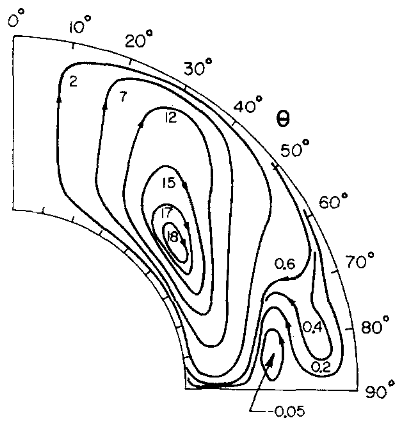

FIG. 4. Contours of $10^4\psi$ for $R = 1000$, $\Omega_1 = 0$, $\Omega_2 = \Omega_0$.

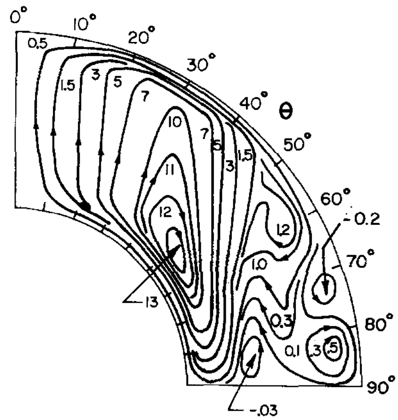

FIG. 5. Contours of $10^4\psi$ for $R = 2000$, $\Omega_1 = 0$, $\Omega_2 = \Omega_0$.

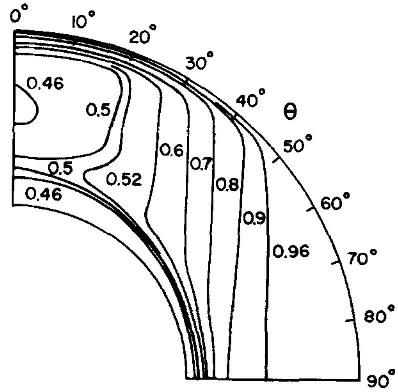

FIG. 6. Contours of angular velocity for $R = 1000$, $\Omega_1 = 0$, $\Omega_2 = \Omega_0$.

$R = 3000$ by Greenspan [11, Fig. 14]. Contours of constant angular velocity for the case $\Omega_1 = 0$, $\Omega_2 = \Omega_0$, $R = 1000$ are given in Fig. 6. These may be compared with those obtained by Pearson [10, Fig. 5] for the corresponding late time solution.

On the whole the above comparisons seem to be satisfactory and tend to confirm that the method is adequate. The series truncation method has the advantage of reducing the problem to the solution of ordinary differential equations but the problem of taking an adequate number of terms n_0 in each of the series must then be faced since the amount of computation increases rapidly as n_0 increases. The main feature of the application discussed in the present paper is the solution of the set of equations (16) subject to (17) by means of step-by-step methods. The method described was found to be extremely rapid and accurate. In all the computed cases described above the final solutions of (16) were found to satisfy (17) to at least eight or nine decimal places. The formulation and method described is applicable to a number of other problems involving rotating fluids and spheres.

Appendix

In terms of the variable $\mu = \cos\theta$ and the associated Legendre functions of the first kind

$$P_n^m(\mu),$$

the Gegenbauer functions satisfy the relations

$$I_{n+1}(\mu) = \frac{(1-\mu^2)^{1/2}}{n(n+1)} P_n^1(\mu), \tag{59}$$

$$I'_{n+1}(\mu) = -P_n(\mu), \tag{60}$$

where the prime denotes differentiation with regard to μ. The orthogonality properties are

$$\begin{aligned} \int_{-1}^{1} \frac{I_m(\mu)\, I_n(\mu)}{1-\mu^2}\, d\mu &= 0, & m \neq n, \\ &= \frac{2}{n(n-1)(2n-1)}, & m = n, \end{aligned} \tag{61}$$

provided neither m nor n is 0 or 1.

On substitution of (59) and (60) in the integral (21) we obtain

$$L(l, m, n) = -\frac{1}{2}\int_{-1}^{1} \frac{P_l^1(\mu)\, P_m^1(\mu)\, P_n(\mu)}{l(l+1)\, m(m+1)}\, d\mu. \tag{62}$$

This integral may be evaluated in terms of the $3 - j$ symbols by introducing the spherical harmonics defined by Talman [20, pp. 164–168] in the form

$$Y_{l,m}(\theta, \phi) = (-1)^m \left[\frac{(l-m)!}{(l+m)!}\right]^{1/2} P_l^m(\mu)\, e^{im\phi}, \tag{63}$$

$$Y_{l,-m}(\theta, \phi) = (-1)^m\, \overline{Y}_{l,m}(\theta, \phi), \tag{64}$$

where the bar denotes the complex conjugate, and utilizing the result

$$\int_0^{2\pi} d\phi \int_0^{\pi} Y_{l,p}(\theta, \phi)\, Y_{m,q}(\theta, \phi)\, \overline{Y}_{n,s}(\theta, \phi) \sin\theta\, d\theta$$

$$= 4\pi(-1)^s \begin{pmatrix} l & m & n \\ p & q & -s \end{pmatrix} \begin{pmatrix} l & m & n \\ 0 & 0 & 0 \end{pmatrix}. \tag{65}$$

It is to be noted that $\left(\begin{smallmatrix} l & m & n \\ p & q & -s \end{smallmatrix}\right)$ is interpreted as zero unless both $| l - m | < n < l + m$ and $s = p + q$, and can also be zero in other individual cases. Result (23) follows at once from (63)–(65).

Finally, result (24) follows in a similar manner by substituting from (59) into integral (22), utilizing the relation

$$\frac{\mu}{(1-\mu^2)^{1/2}} P_n^1(\mu) = -\frac{1}{2}\left[P_n^2(\mu) + n(n+1)\, P_n(\mu)\right] \tag{66}$$

and applying results (63)–(65).

Acknowledgments

The calculations were carried out on the CYBER 73 of the University of Western Ontario. The work was supported by a grant from the National Research Council of Canada.

References

1. H. Bondi and R. A. Lyttleton, *Proc. Cambridge Phil. Soc.* **44** (1948), 345.
2. I. Proudman, *J. Fluid Mech.* **1** (1956), 505.
3. G. F. Carrier, *J. Fluid Mech.* **23** (1965), 145.
4. K. Stewartson, *J. Fluid Mech.* **26** (1966), 131.
5. J. Pedlosky, *J. Fluid Mech.* **36** (1969), 401.
6. W. L. Haberman, *Phys. Fluids* **5** (1962), 625.
7. Iu. G. Ovseenko, *Isv. Vyssh. Ucheb. Zaved., Matematika* **35** (1963), 129.
8. W. E. Langlois, *Quart. Appl. Math.* **21** (1963), 61.
9. B. R. Munson and D. D. Joseph, *J. Fluid Mech.* **49** (1971), 289.
10. C. E. Pearson, *J. Fluid Mech.* **28** (1967), 323.
11. D. Greenspan, *Computers & Fluids* **3** (1975), 69.
12. M. D. van Dyke, Proc. 11th Int. Cong. Appl. Mech. (Munich, 1964), 1165.
13. M. D. van Dyke, Stanford University SUDAER no. 247, 1965.

14. R. L. Underwood, *J. Fluid Mech.* **37** (1969), 95.
15. S. C. R. Dennis and J. D. A. Walker, *J. Fluid Mech.* **48** (1971), 771.
16. S. C. R. Dennis and Gau-Zu Chang, *J. Fluid Mech.* **42** (1970), 471.
17. W. M. Collins and S. C. R. Dennis, *J. Fluid Mech.* **60** (1973), 105.
18. R. A. Sampson, *Phil. Trans. Roy. Soc. London, Ser. A* **182** (1891), 449.
19. J. Happel and H. Brenner, "Low Reynolds Number Hydrodynamics," pp. 134–138, Prentice-Hall, Englewood Cliffs, N.J., 1965.
20. J. D. Talman, "Special Functions," Chap. 9, Benjamin, New York, 1968.
21. M. Rotenberg, M. Bivins, N. Metropolis, and J. K. Wooten, "The 3-*j* and 6-*j* Symbols," M.I.T. Press, Cambridge, Mass., 1959.
22. J. B. Rosser, Mathematics Research Center, University of Wisconsin, Technical Summary Report No. 797, 1967.
23. S. C. R. Dennis and Gau-Zu Chang, Mathematics Research Center, University of Wisconsin, Technical Summary Report No. 859, 1969.